Pertanika J. Sci. & Technol. 30 (4): 2747 - 2766 (2022)

PERTANIKA JOURNALS

SCIENCE & TECHNOLOGY

Journal homepage: http://www.pertanika.upm.edu.my/

The Kinetic Evaluation and DFT Study of Cis-[Pt(Asc)(NH_3)$_2$] Complex as an Inhibitor to Type 2 Diabetic Human Amylase

Khalid Farouk Al-Rawi[1], Khaldoon Taher Maher[2], Othman Ibrahim Alajrawy[3]* and Firas Taher Maher[4]

[1]*Department of Chemistry, College of Science, University of Anbar, 00964 Iraq*
[2]*Al-Amal National Hospital for Cancer Management, Baghdad 00964 Iraq*
[3]*Department of Applied Chemistry, College of Applied Science, University of Fallujah, 00964 Iraq*
[4]*Department of Chemistry, College of Science, Tikrit University, Tikrit 00964 Iraq*

ABSTRACT

Several metal complexes and organic compounds and extracted herbs that might be involved in the bio-mechanism of the type 2 diabetes mellitus treatments. This research aims to synthesize a new platinum (II) complex and study its kinetics as an inhibitor for freshly purified amylase from type 2 human diabetics. The amylase enzyme was precipitated from diabetic patients. The complex cis- [Pt(Asc)(NH_3)$_2$] was synthesized and characterized experimentally and theoretically by DFT calculations to conclude the structure. Both calculations confirmed the square planar geometry for the prepared complex. The results showed that the complex is more stable and polar than the L-ascorbic acid derivative. Therefore, we suggested that the synthesized Pt(II) complex is appropriate to be examined as an inhibitor for the amylase enzyme. Several concentrations from the Pt(II) complex were prepared for kinetic purposes. Kinetic results have shown that the newly prepared complex has a remarkable inhibition effect on the amylase enzyme. Kinetic parameters were fitted using the Lineweaver–Burk plot. The inhibition reaction was confirmed as a non-competitive inhibitor. Also, an inorganic compound derived from vitamin C was prepared and diagnosed by several spectroscopic methods, and a comparison between the experimental and theoretical data was conducted. The DFT study of the prepared complex gave a useful explanation for the complex and its stability. Thus, an

ARTICLE INFO

Article history:
Received: 10 November 2021
Accepted: 05 April 2022
Published: 23 September 2022

DOI: https://doi.org/10.47836/pjst.30.4.25

E-mail addresses:
sc.kfwi72@uoanbar.edu.iq (Khalid Farouk Al-Rawi)
khaldontaher@gmail.com (Khaldoon Taher Maher)
othman-ibrahimasc@uofallujah.edu.iq (Othman Ibrahim Alajrawy)
Firastaher3@gmail.com (Firas Taher Maher)
* Corresponding author

ISSN: 0128-7680
e-ISSN: 2231-8526

inhibitory effect on the activity of the amylase enzyme was clearly shown by the newly prepared Pt(II) complex. It can be concluded that Pt(II) complex could be used as an amylase inhibitor.

Keywords: Amylase, cisplatin, inhibition complex, L-ascorbic acid, platinum complexes, T2DM, theoretical calculation

INTRODUCTION

Diabetes mellitus is a chronic disease when the pancreas cannot generate enough insulin (Ard et al., 2020). It also occurs when the body is unable to successfully consume the produced insulin (Halim & Halim, 2019). It is well known that insulin is a regulatory hormone for the sugar level in the blood. The symptom of hyperglycemia or hypoglycemia is uncontrolled diabetes which can cause severe impairment to some organs, such as nerves and vessels of the blood (Egan & Dinneen, 2019).

The digestion of the carbohydrates into small sugar molecules such as glucose starts with the amylase enzyme (Association, 2014). A human amylase is an enzyme that has the following commission number E.C. 3.2.1.1 (EFSA Panel on Food Contact Materials et al., 2020). The main function of amylase is to digest carbohydrates molecules into smaller subunits (Kumar & Chakravarty, 2018). There are two main types of the amylase enzyme, salivary and pancreatic, found in some fungi, bacteria, and plant seeds (Hong et al., 2019; López et al., 2018; Whitcomb & Lowe, 2007). The amylase enzyme produced from saliva is used to hydrolyze internal α-1,4-glycosidic linkages in starch in low molecular weight products, such as maltose, glucose, and maltotriose units (Yu, 2019). The pancreatic amylase is associated with the digestion of starch. This enzyme is found in the blood, helping in digesting the dead white blood cells (Chen et al., 2019). The amylase enzyme can be used to produce corn syrup in high-fructose concentration and alcohol. It is also used to facilitate the digestion of animal food, as well as in the yeast industry (Burhan et al., 2003).

However, the more digested carbohydrate in the body and sugar absorbed, the more chances for hyperglycemia and diabetes mellitus risks. Therefore, amylase inhibition would be a good way to decrease sugar production in the body (Oboh et al., 2014). Several studies have suggested various metal complexes, synthesized organic compounds, and plant extracts involved in the amylase inhibition mechanisms (Bergamini et al., 2008). We have coordinately synthesized a new platinum (II) complex using L-ascorbic acid as a ligand. This complex was synthesized, characterized by different spectroscopic techniques, and finally examined by computational studies utilizing density functional theory (DFT). It is suggested that the platinum complex may bind to an active site of the enzyme or another site which affects the binding of substrate to the enzyme's active site, leading to amylase inhibition (Mahmood, 2016).

The metal ascorbates complexes had previously shown beneficial biological applications. First, they were used for treating symptoms related to vitamin C and metal ion deficiencies. Secondly, metal ascorbates had been previously utilized to develop some therapeutic agents used as potential anticancer, antibacterial, antioxidant, and antihypoxic (Bradshaw et al., 2011; Romero-Canelon & Sadler, 2013). In addition, metal ascorbates were also used as synthetic models for some metal-containing biological systems. Studies have investigated the bioactivity of the metal ascorbate complexes such as *Cis*-diamineplatinum (II) ascorbate complexes. These studies confirmed the activity of these complexes in the anticancer prodrugs (Hollis et al., 1987). *Cis*-diamineplatinum (II) ascorbate complexes had revealed antitumor activity (Hollis et al., 1987). Similar complexes had been identified as the best-found metal involving the drug. $[Pt(phen)_2]^{+2}$ had shown a remarkable inhibiting effect on tumor cells (Zümreoglu-Karan, 2006). Another well-identified complex is phenanthroline ascorbates which had been revealed as an anticancer drug. Other researchers synthesized complexes as anticancer (Czarnomysy et al., 2018), antineoplastic activities (Yαlçın, 1995), and antiproliferative activity (Bergamini et al., 2008).

MATERIALS AND METHODS

Subjects

Patients. One hundred diabetic patients and 100 healthy individuals were recruited as a control group throughout the study from December 2019 to the end of March 2020 in Tikrit Teaching Hospital, Tikrit, Iraq. The research was registered by the Research Ethics Committee of the Iraqi Ministry of Health, Iraq. Ten milliliters of blood were collected into a test tube without anticoagulants. Blood samples were left for 20–30 minutes at 37 °C. The serum was obtained by blood centrifugation at 4000 rpm (1814 × g) for 10 min, and then the serum was used for the kinetic assays. Amylase was estimated using amylase Kits from BIOLABO Company-BIOLABO SAS-AMYLASE (NPG3: Liguid reagent) REF.LP99553, the French manufacturer of Reagents for Medical Biology, France, uses the colorimetric method.

Purification of Amylase

The following procedure was used to purify amylase: $(NH_4)_2SO_4$ (60%), 12 g was added to precipitate amylase (Duong-Ly & Gabelli, 2014). The precipitate was dissolved in a Tris-HCl buffer pH 7.0 and dialyzed out of salt using a buffer solution pH 6.0. Next, an Ion-exchange (I.E) type Diethylaminoethyl-Sephacel (DEAE-Sephacel) was used for further purification and to make the enzyme more concentrated with a flow rate of 2 ml/4 min (Albuquerque et al., 2016). Then the product was loaded to the gel filtration chromatography (G.L) column type Sephadex G50, pH: 6, with a flow rate of 2 ml /min on

column 30 × 2.5 cm to confirm the molecular weight of the enzyme (Zhao et al., 2018). All materials were purchased from BDH and Fluka Companies. The electrophoresis technique was finally used to confirm the purity and the molecular weight of the amylase enzyme using polyacrylamide gel on SDS-PAGE. The electrophoresis adopted in this study was carried out with a current of 30 mA, and the gel was stained with a Coomassie brilliant blue R – 250 (Hames, 1998).

Preparation of the Compounds

Preparation of the L-ascorbic acid derivative and the cis-[Pt(Asc)$(NH_3)_2$] complex was carried out according to the methods described in previous studies (Salomon, 1963).

Effect of the New Inhibitors

The Pt(II) compound was measured at different concentrations ranging from 5×10^{-1} to 5×10^{-8} g/25 ml. In addition, the type of inhibition was studied with a sequential concentration of the substrate 0.5−5 mM and a single concentration of Pt(II) complex 0.005 g/25 ml. Finally, a Lineweaver–Burk plot was applied to obtain the *Km*, the *Vmax,* and the inhibition type.

Statistical Analysis

The biochemical data were analyzed statistically using the Graph Pad Prism software 7.04 (USA). ANOVA was performed to estimate the mean ± standard deviation (SD, and statistical significance was considered whenever the P value was equal to or less than 0.05.

Theoretical Calculations

The density functional theory (DFT) calculations were done using the package of Gaussian 09W software with different basis sets DFT-B3LYP/6-31G for the (Asc) derivative, whereas LanL2DZ was used for the complex preparations.

RESULTS AND DISCUSSION

Biochemical Study

This study showed a significant increase in the level of amylase enzyme reaching 270 ± 5.32 U/L for patients, while the amylase activity in the control group was 105 ± 3.24 U/L. The enzyme leakage caused this increase from the pancreatic channel to the blood instead of the intestine (Tilley & Smith Jr, 2015). The amylase enzyme levels in chronic pancreatitis were lower than in acute pancreatitis but higher than normal. The normal level of acute pancreatitis was temporary and narrow for 8–72 hours, whereas the level of the enzyme was the highest in 24–30 hours from the onset of the disease. It happened in case of levels rise to 550 units and sometimes 2,000 units and continue to increase. A few days

later, the levels decreased due to the enzyme's ability to leak through the kidneys into the bloodstream. Blood samples were used to detect the efficacy of the amylase enzyme. The samples were collected from the patients in a short period to obtain a reliable diagnostic tool (Varley et al., 1988).

Purification of Amylase

Table 1 shows the purification of the amylase enzyme using several steps. Firstly, $(NH_4)_2SO_4$ salt 60% was used to precipitate the amylase to obtain 1.21 folds of purification, yielding 83%, and specific activity (S.A) was 10.74 IU/mg. Secondly, dialysis gave 1.99 folds of the purification process. The final yield was about 71%, and the S.A was 21.37 IU/mg. Next, ion exchange chromatography was applied to indicate one band of the purified enzyme with 4.25 folds. The final yield percentage of this step was 52%, and S.A was 37.57 IU/mg. Finally, gel filtration chromatography was applied to obtain 4.31 folds of purification, and the final yield was 35.5%, whereas the S.A was 38.18 IU/mg.

Table 1
Partial purification of amylase from the serum of type 2 diabetic patients using ammonium sulfate, ion-exchange, and gel filtration chromatography

Yield %	Folds of Purification (time)	Specific activity (IU/mg)	Total protein (mg)	Protein conc. (mg/mL)	Total activity (IU)	Activity (IU/mL)	Elute mL	Step
100	**1**	**8.84**	**266.8**	**13.34**	**2360**	**118**	**20**	**Crude portion**
83	**1.21**	**10.74**	**145.92**	**9.12**	**1568**	**98**	**16**	**Ammonium Sulfate**
71	**1.99**	**21.37**	**43.23**	**3.93**	**924**	**84**	**11**	**Dialysis**
52	**4.25**	**37.57**	**8.25**	**1.65**	**310**	**62**	**5**	**Ionic Exchange**
35.5	**4.31**	**38.18**	**4.3**	**1.1**	**168**	**42**	**4**	**Gel filtration**

Electrophoresis of the purified amylase from human red blood cells showed one protein band appearing on the SDS-PAGE at the exact molecular weight, (45.20) kDa, compared to standards (Markers) by fitting the results of log M.Wt. against relative mobility as shown in Figure 1. It represents the amylase enzyme obtained after the ion exchange and gel filtration chromatography.

Marker lane refers to proteins marker with different molecular weights (commercial). Extracted lane refers to the enzyme after extractions. +AS lane refers to the enzyme after extracting by ammonium sulfate. The lane labeled with +IXE refers to amylase enzyme after ion exchange column with impurities; Wash 1 and 2 lanes: the fractionated volumes after washing IXE column. L lane: Load of the extract to the column, +G.F Lane shows the purified amylase after the gel filtration step.

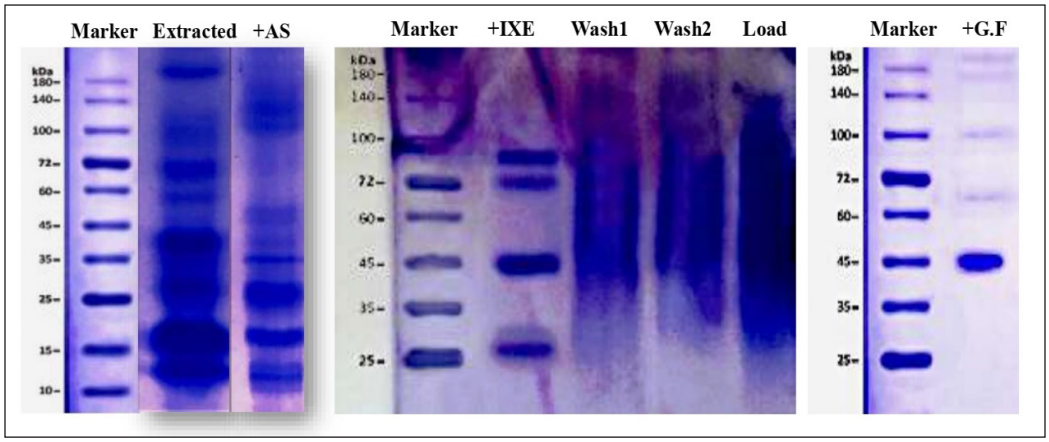

Figure 1. Electrophoresis of the purified amylase enzyme from human red blood cells with polyacrylamide gel

Kinetic Study of a Partially Purified Amylase Enzyme

The results showed an increase in the amylase activity with an increase in the substrate concentration. The *Vmax* of amylase enzymes was calculated at the optimal substrate concentration of 6 mmol using the Michaelis-Menten model showing a hyperbolic curve (Figure 2). The velocity of the amylase enzyme tested by the Lineweaver–Burk model showed that *Km* was 10.914 mM and *Vmax* was 34.25 IU/L (Figure 3). The maximum temperature at which amylase showed bioactivity was 60 °C (Figure 4). Regarding the effect of the pH on amylase activity, the optimum pH was 7.3. We noticed that when pH

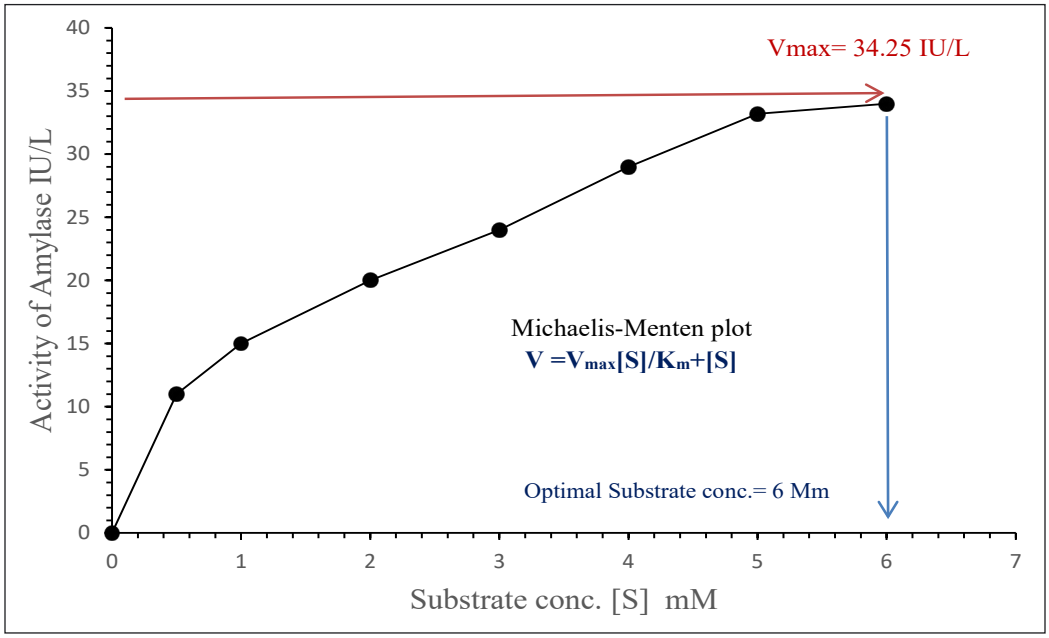

Figure 2. The relationship between the amylase activity and the substrate concentration

increases, the enzyme's activity increases until it reaches the maximum pH, whereby the enzyme could be denatured after this point (Figure 5). However, the activity was increased with time to the maximum of 37 °C after 40 minutes. We noticed that when the temperature increases, the enzyme's activity still increases until it reaches the maximum temperature for the same reason (Figure 6). These results confirmed previous studies about the maximum temperature and the best pH where amylase still shows bioactivity (Al-Qodah, 2007; Adnan, 2010; Mohhmod, 2010; Dhote et al., 2014).

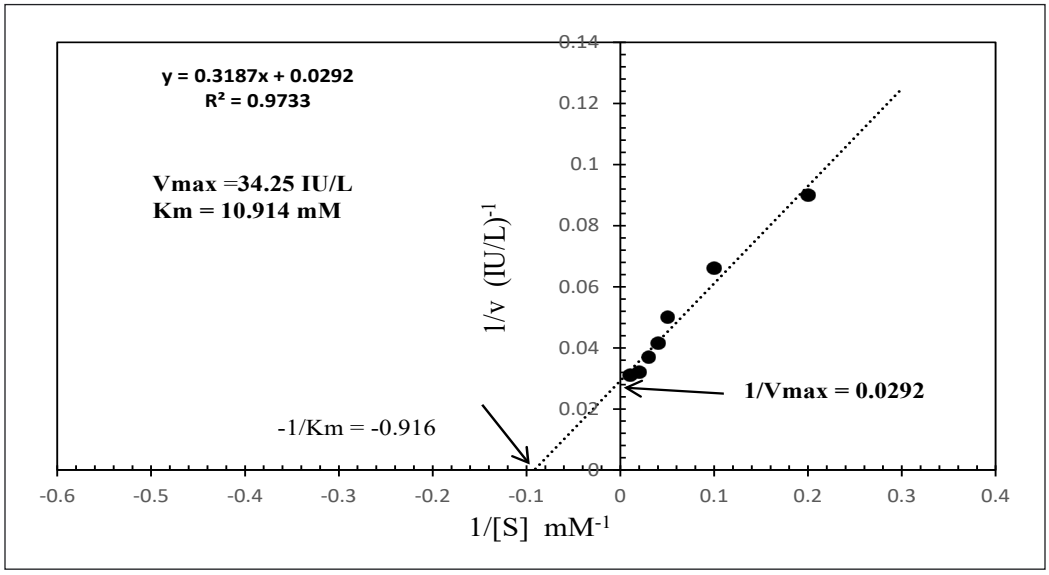

Figure 3. Lineweaver–Burk plotting 1/v versus 1/[S] of purified amylase

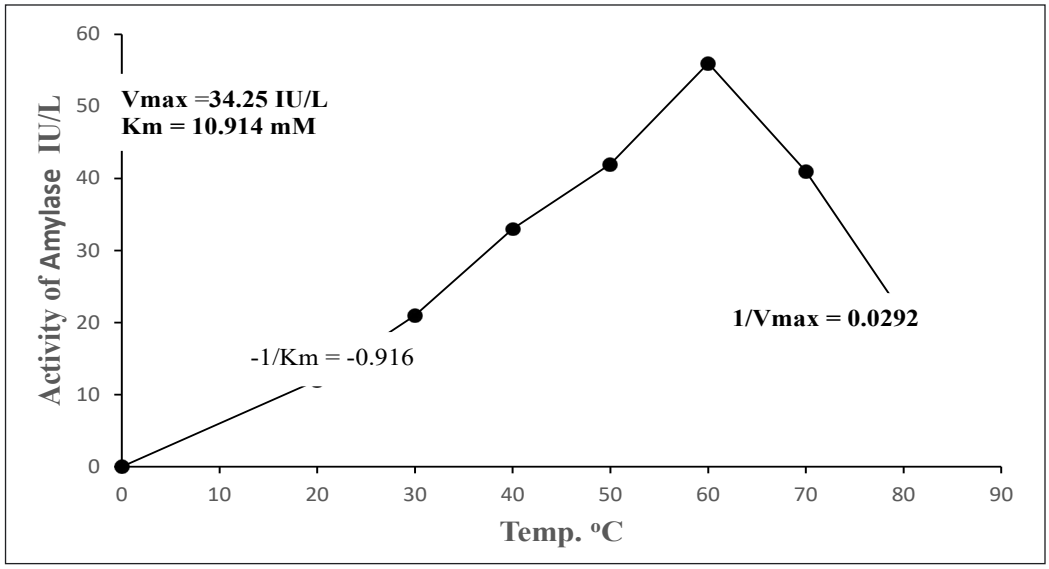

Figure 4. Effect of temperature on amylase activity

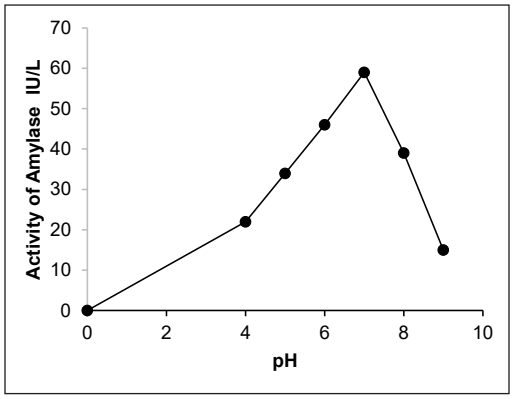

Figure 5. Effect of pH on amylase activity

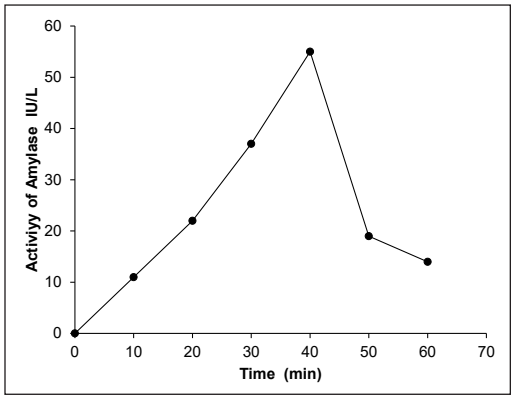

Figure 6. Incubation time of substrate with purified amylase at 25 °C and pH 7

Preparation of 5,6-O-isopropylidene-L-Ascorbic Acid

The L-ascorbic acid molecule has four hydroxyl groups; these groups are active for classical esterification (Figure 7). The synthesis of the derivative occurred in 2 and 3-positions. The first conversion into its 5,6-isopropylidene derivative happened because the carbon-6 hydroxyl group (a primary hydroxyl group) is the most reactive. The acetal is stable in alkaline conditions but readily hydrolyzed by dilute acid (Maher et al., 2017). Hence, it is very useful as a blocking agent. It was used in this work to protect the hydroxyl group at C-5 and C-6, whereas leaving the hydroxyl groups at C-2 and C-3 free for the required chemical modification. According to the literature, the L-ascorbic acid derivative was prepared from the reaction of L-ascorbic acid with acetone in acidic media (Salomon, 1963).

The FTIR spectra of the L-ascorbic acid derivative are depicted in Figure 8. The stretching bands at 3244 cm^{-1} are assigned for ν(O-H), 2995 cm^{-1} for ν(C-H aliphatic), 1755 cm^{-1} for ν(C=O) lactone, 1664 cm^{-1} for ν(C=C), and 1141 cm^{-1} for ν(C-O). The calculated spectrum was performed to make a comparison with the experimental one. The obtained data are acceptable with the experimental data; the stretching of the ν(O-H) appeared at 3455, the stretching of the ν(C-H aliphatic) at 3135, the stretching of the ν(C=O) lactone

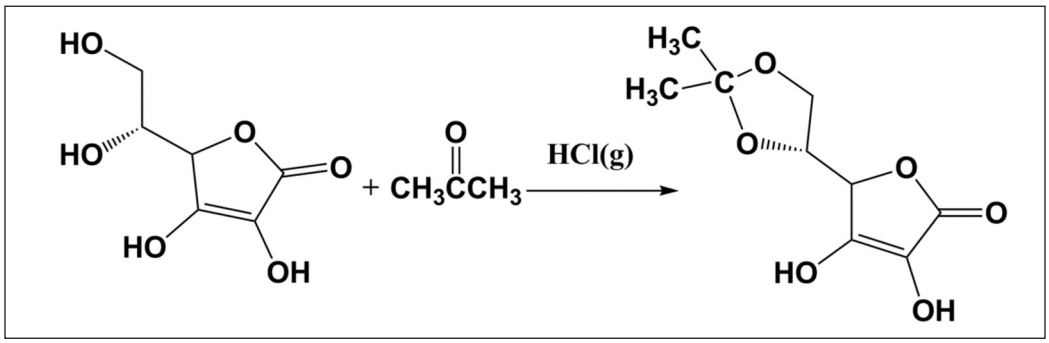

Figure 7. The preparation of L-ascorbic acid derivative

at (1888), the stretching of the ν(C=C) at 1789 and finally the stretching of the ν(C-O) at 1172 (Table 2).

The ^{1}H-NMR spectrum of L-ascorbic acid derivative Figure 9, showed a singlet signal at 11.27 ppm, which belongs to the proton of the (OH) hydroxyl group at C–2. The singlet signal at 8.46 ppm belongs to the proton of the (OH) hydroxyl group at C–3, and the doublet signal at 4.71 ppm belongs to the proton of the (H-C4). The quartet signal at

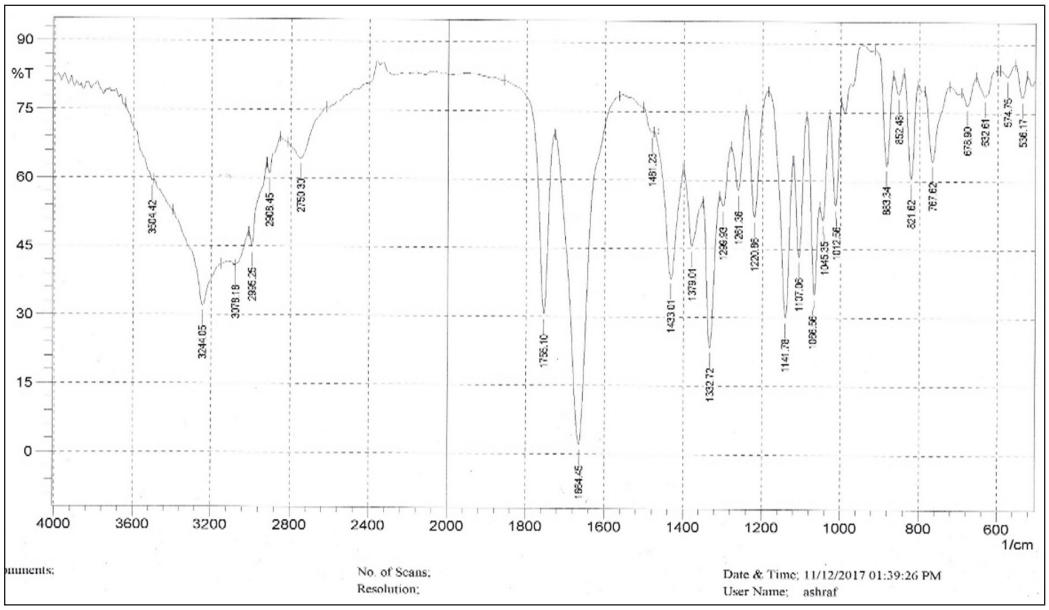

Figure 8. The experimental FTIR spectrum of L-ascorbic acid derivative

Table 2
Observed and calculated vibrational frequencies cm^{-1} for L-ascorbic derivative ligand and Pt (II) complex

Compound	Obs.	Calc.	Assignment
L-ascorbic derivative Ligand	3244	3720	υ(O-H)
	2995	3135	υ(C-H)
	1755	1888	υ(C=O)
	1644	1789	υ(C=C)
	1144	1172	υ(C-O)
	-	-	υ(O-H)
Pt-ASCA complex	3251	3591	υ(N-H)
	2981	3127	υ(C-H)
	1743	1774	υ(C=O)
	1612	1664	υ(C=C)
	1139	1334	υ(C-O)
	574	571	υ(M-O)
	468	472	υ(M-N)

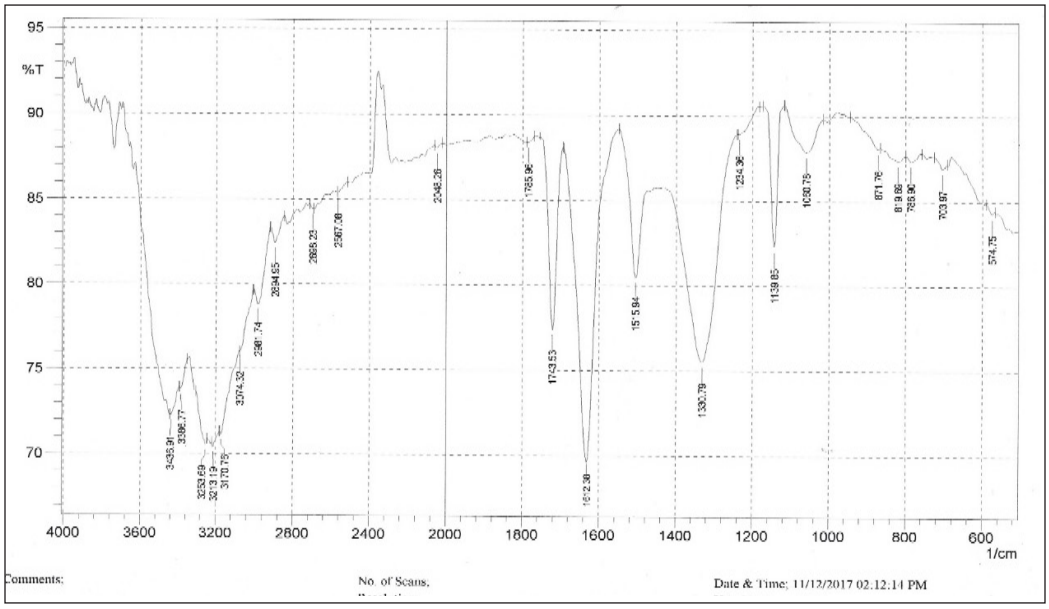

Figure 9. The ^{1}H-NMR spectrum of L-ascorbic acid derivative

4.26 ppm belongs to the proton of the (H-C5), and the doublet signal at 4.11 ppm belongs to the proton of the (H-C6). The doublet signal at 3.89 ppm belongs to the proton of the (H-C6), and the singlet signal at 1.26 ppm belongs to the proton of the aliphatic 2(CH_3) (Silverstein et al., 2005; Mistry, 2009). These data have been compared with the calculated data, which showed an acceptable difference between the two results. The deviation between the obtained data may be attributed to the different ways to get the data.

Synthesis of the Complex Cis-[Pt(Asc)(NH_3)$_2$]

The complex was prepared by the reaction of the ligand with cis-[Pt(Cl)$_2$(NH_3)$_2$] solution, as shown in Figure 10. The FTIR spectrum of the cis-[Pt(Asc)(NH_3)$_2$] complex is depicted in Figure 11. The spectrum showed stretching bands at 3213, 3253 cm^{-1} assigned for ν(NH_3),

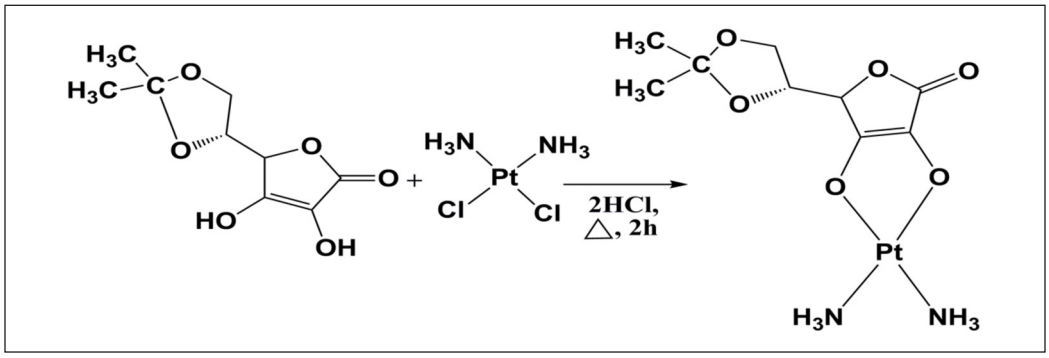

Figure 10. The reaction of the L-ascorbic acid derivative ligand with cis-[Pt(Cl)$_2$(NH_3)$_2$]

2981 cm^{-1} for ν(C-H aliphatic), 1743 cm^{-1} for ν(C=O) lactone, 1612 cm^{-1} for ν(C=C), 1139 cm^{-1} for ν(C-O). The ^{1}H-NMR spectrum of the cis-[Pt(Asc)$(NH_3)_2$] showed a singlet signal at 4.35 ppm, which belongs to the protons of the (NH_3) (Figure 12). The doublet signal at 4.21 ppm belongs to the proton of the (H-C4), and a quartet signal at 3.9 ppm belongs to the proton of the (H-C5). The doublet signal at (3.78-3.7 ppm) belongs to the protons of the (2H-C6), and the singlet signal at 1.25 ppm belongs to the protons of the aliphatic $2(CH_3)$ (Silverstein et al., 2005; Mistry, 2009).

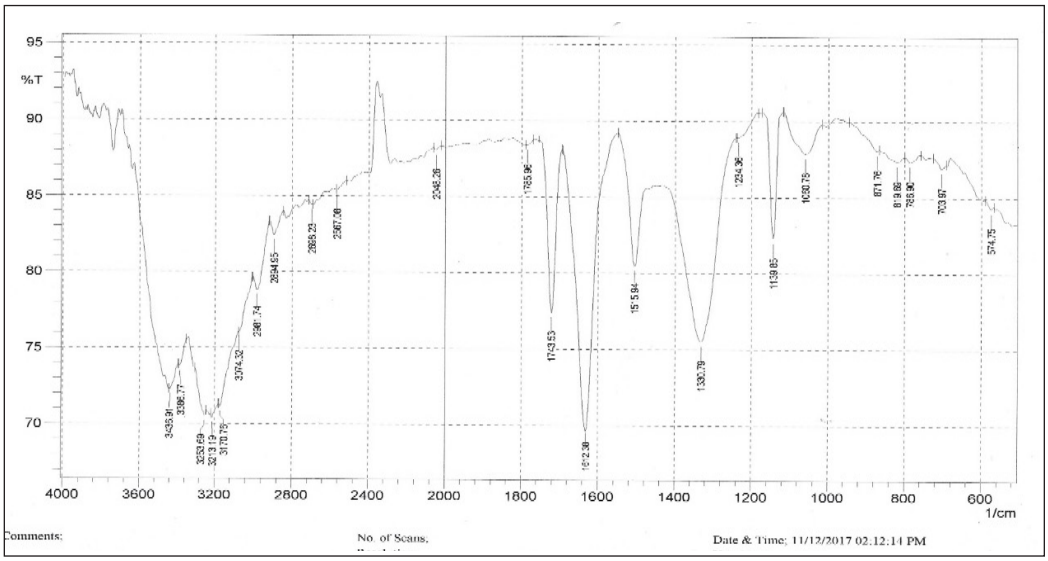

Figure 11. The experimental FTIR spectrum of the complex cis-[Pt(Asc)$(NH_3)_2$]

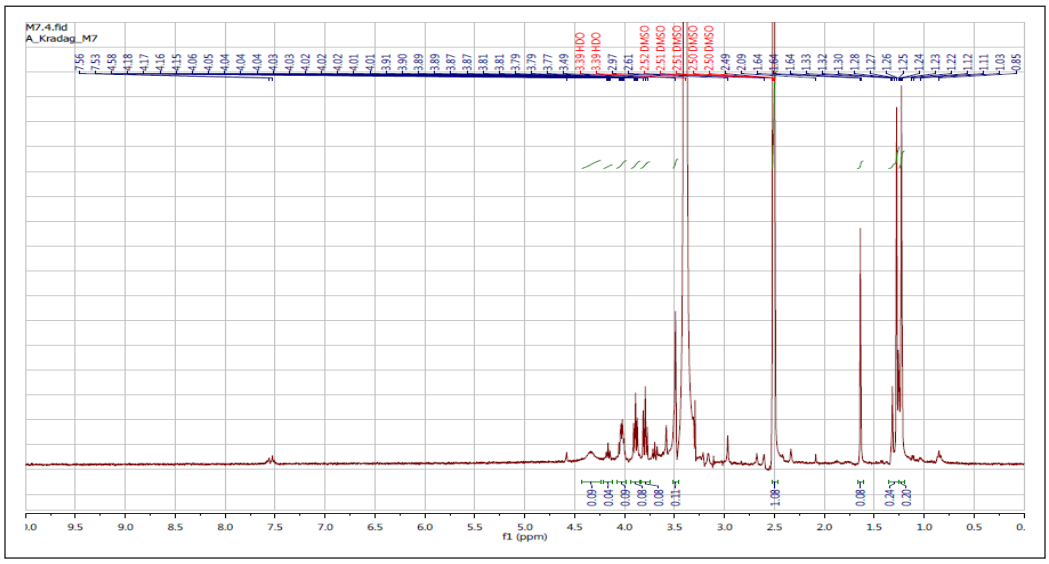

Figure 12. The ^{1}H-NMR spectrum of the complex cis-[Pt(Asc)$(NH_3)_2$]

DFT Calculations

The molecular geometries of the L-ascorbic acid derivative, the cisplatin, and the prepared Pt(II) complex were fully optimized using G 09W (Chattaraj & Poddar, 1999; Caruso et al., 2012; Sabounchei et al., 2015; Ali et al., 2019). The optimized structures and natural bond charges are presented in Figure 13. Structural data are given in Table 3. The angles around the Pt(II) atom ranged from 81.82° to 105.83°, and the two dihedral angles are 172.43° to 169.53°. These angles deviated from the perfect square planar geometry, suggesting the distorted structure for the Pt(II) complex, whereby the O-Pt-O bond angle was 87.71°. Compared with the literature on platinum(II) complexes, the bond angle was 84.36° in [Pt(N, N-dimethyl-N'-(2H-1,2,4-triazole-3-yl) formamidine)ox].2H_2O (Soliman et al., 2016), and the N-Pt-N bond angle was 105.83. The Pt-O bond lengths found 2.020-2.042 Å

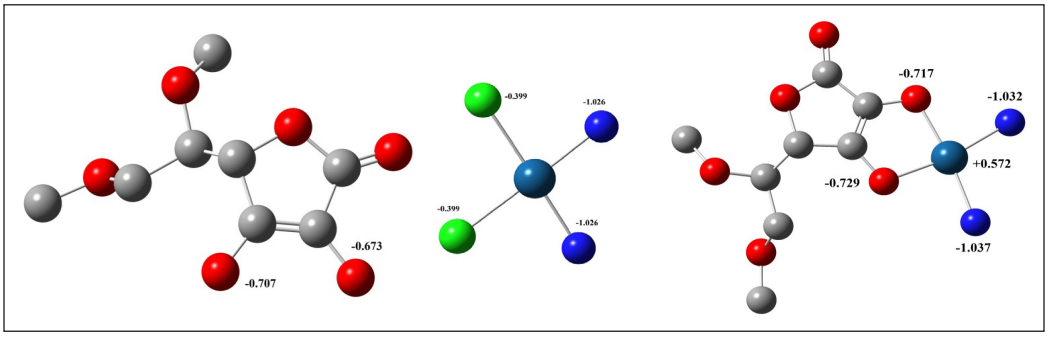

Figure 13. The optimized structures and natural bond charges of the studied compounds. The hydrogen atoms have been omitted for simplicity

Table 3
Bond lengths (Å), bond angles (°), and dihedral angles (°) of optimized cisplatin and Pt(II) complex using the DFT/B3LYP/Lan2DZ basis set

Cisplatin °A	Bond Lengths		Bond Angles °
Pt(1)-N(2)	2.110	N(2)-Pt(1)-N(5)	99.30
Pt(1)-N(5)	2.110	Cl(10)-Pt(1)-Cl(11)	96.71
Pt(1)-Cl(10)	2.410	N(2)-Pt(1)-Cl(10)	81.98
Pt(1)-Cl(11)	2.410	N(5)-Pt(1)-Cl(11)	81.99
		N(2)-Pt(1)-Cl(11)	178.70
		N(5)-Pt(1)-Cl(10)	178.70
Pt-ASCA complex			
Pt(25)-O(1)	2.042	O(1)-Pt(25)-O(10)	87.71
Pt(25)-O(10)	2.020	N(26)-Pt(25)-N(29)	105.83
Pt(25)-N(26)	2.100	N(26)-Pt(25)-O(10)	81.83
Pt(25)-N(29)	2.115	N(29)-Pt(25)-O(1)	84.63
		N(29)-Pt(25)-O(10)	172.34
		N(26)-Pt(25)-O(1)	169.53

are consistent with the range of reported values of 2.016 (Bakalova et al., 2009; Mansour, 2013; Soliman et al., 2016). The charge densities distributed on L-ascorbic acid derivative ligand oxygen atoms explain their expected donor properties (Chattaraj & Poddar, 1999). Platinum has a positive charge of +0.572 and acts as the acceptor. The back donation of electrons from Pt(II) to the L-ascorbic acid derivative ligand is assumed from the increase of the negative charges on the oxygen atoms. It is an MLCT from the Pt(II) to the π* orbitals of the L-ascorbic acid derivative ligand. The Pt(II) complex 15.788 Debye is more polarized than the L-ascorbic acid derivative ligand 6.489 Debye, whereas, for cisplatin 11.719, the electronic energy of the Pt(II) complex is (-994.402 a.u.). It confirmed that the complex is more stable than the ligand (-763.372 a.u.) and the cisplatin 262.298 a.u. (Sabounchei et al., 2015). HOMO and LUMO energies of the L-ascorbic acid derivative, the cisplatin, and the Pt(II) complex are given in Table 4. The hardness is ($\eta=(I-A)/2$), A is the electron affinity, I is the ionization energy, and (I-A) is the difference between the HOMO and the LUMO orbitals (Sabounchei et al., 2015). The higher the value of the gap between the HOMO and the LUMO, the harder the molecule. The η values and ΔE are given in Table 4. The transition is easier in the Pt(II) complex than in the ligand and the cisplatin; the ΔE of the complex is 0.133, the ligand is 0.205, and the cisplatin is 0.161 (McGuire et al., 1984; Bakalova et al., 2009; Mansour, 2013; Elghalban et al., 2014; Sabounchei et al., 2015; Soliman et al., 2016; Ali et al., 2019) and hence the complex is softer (η= (0.006) than in the ligand 0.102 and the cisplatin 0.080) (Chattaraj & Poddar, 1999). The electronic energy and the dipole moments are tabulated in Table 4. The plots of the HOMO and the LUMO for the complex and the L-ascorbic acid derivative ligand are presented in Figure 14.

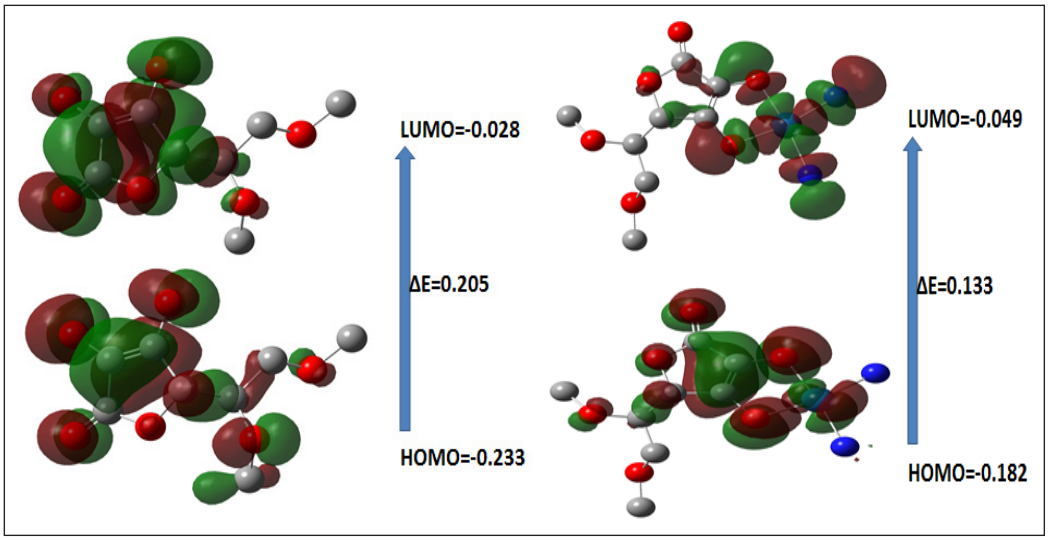

Figure 14. The isodensity surface plots of the HOMO and the LUMO for the Pt(II) complex (right) and the L-ascorbic acid derivative ligand (left). The hydrogen atoms have been omitted for simplicity.

Table 4
The calculated quantum chemical parameters of the L-ascorbic derivative ligand, cisplatin, and Pt(II) complex

Compound	HOMO	LUMO	η	ΔE	Total energy a.u	D.M Debye
L-ascorbic derivative Ligand	-0.233	-0.028	0.102	0.205	-763.37	6.45
Cisplatin	-0.230	-0.069	0.080	0.161	-262.29	11.71
Pt-ASCA complex	-0.182	-0.049	0.066	0.133	-994.40	15.78

The electronic energy of the complex is (-994.402 a.u.), indicating that the complex is more stable than the ligand (-763.372 a.u.) and the cisplatin (-262.29 a.u.) (Chattaraj & Poddar, 1999). Analysis of the natural bond orbital for Pt(II) complex showed the electronic configuration of Pt to be [core] $6s^{0.54}\,5d^{8.62}\,6p^{0.08}\,6d^{0.01}\,6p^{0.18}$, core = 67.993, valence = 9.418 and Rydberg = 0.016, which give total electrons= 77.428 and the charge on Pt is +0.571e(Bakalova et al., 2009). The 5d orbitals are d_{xz} 1.814; d_{xy} 1.691; d_{yz} 1.930; $d_{x^2-y^2}$ 1.296 and dz^2 1.884. The 5d-electron is (8.615) Table 5. The molecular electrostatic potential (MEP) of the L-ascorbic acid derivative ligand, the Pt(II) complex, and cisplatin are shown in Figure 15. The red regions represent (electrophilic reactivity) and the blue regions (nucleophilic reactivity), respectively. The oxygen atoms (red negative) in the L-ascorbic derivative ligand confirmed the reactive sites for the electrophilic attack (McGuire et al.,

Table 5
The electronic configuration, populations of 4d-orbitals and platinum, oxygen, and chloride charge in the cisplatin and Pt (II)-L-ascorbic acid complexes

Compound	Electronic arrangement	d_{xy}	d_{xz}	d_{yz}	$d_{x^2-y^2}$	dz^2	Rydberg electrons	Charge Pt	Charge O and Cl
Cisplatin	[core] $6s^{0.57}$ $5d^{8.80}\,6p^{0.22}$ $6d^{0.01}\,7p^{0.16}$	0.963	1.986	1.990	1.980	1.874	0.019	+0.251	-0.399,Cl -0.399 Cl
Pt(II)-ASCD complex	[core] $6s^{0.54}$ $5d^{8.62}\,6p^{0.08}$ $6d^{0.01}\,7p^{0.18}$	1.691	1.814	1.930	1.296	1.884	0.016	+0.571	-0.927 O -0.917 O

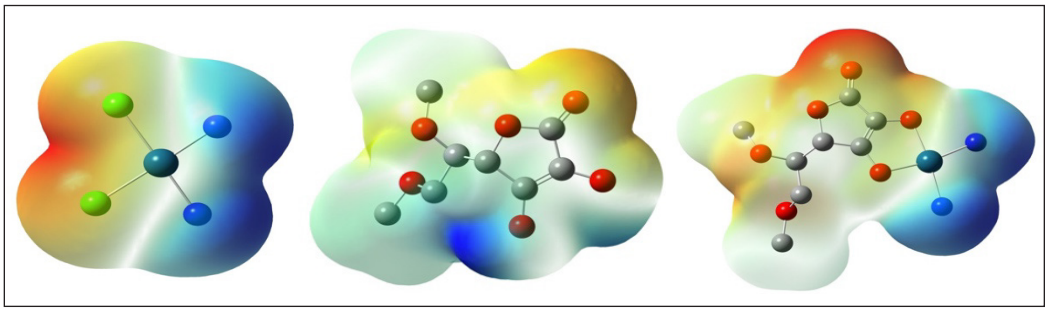

Figure 15. The MEP (molecular electronic potential) of the L-ascorbic acid derivative ligand, the cisplatin, and the Pt(II) complex. The hydrogen atoms have been omitted for simplicity.

1984; Bakalova et al., 2009; Mansour, 2013; Elghalban et al., 2014; Sabounchei et al., 2015; Soliman et al., 2016; Ali et al., 2019).

Effect of the New Inhibitors

The effect of the prepared Pt(II) complex on the purified amylase enzyme activity is illustrated in Table 6. The newly prepared Pt(II) complex's inhibitory effect on amylase enzyme was examined *in vitro*. The results showed that the inhibitory effect of the amylase enzyme increases with the increase of complex concentrations. The activity (without inhibitor) was 78.68± 6.62U/L. The activity with the complex (inhibitors) ranged from 23.81±2.29 to 76.45±5.76 U/L. At the concentrations of 5×10^{-6} mg/25 ml and 5×10^{-7} mg/25 ml, it was found that the activity

Table 6
The inhibitory effect of the compound on amylase activity

Concentrations	Amylase Activity U/L Compounds
Normal/without any concentrations of complex	78.68±6.62
0.5 mg/25ml	23.81±2.29
0.5×10^{-1} mg/25ml	34.13±2.98
0.5×10^{-2} mg/25ml	46.21±3.38
0.5×10^{-3} mg/25ml	52.13±4.11
0.5×10^{-4} mg/25ml	60.24±4.81
0.5×10^{-5} mg/25ml	66.40±5.27
0.5×10^{-6} mg/25ml	76.45±5.76

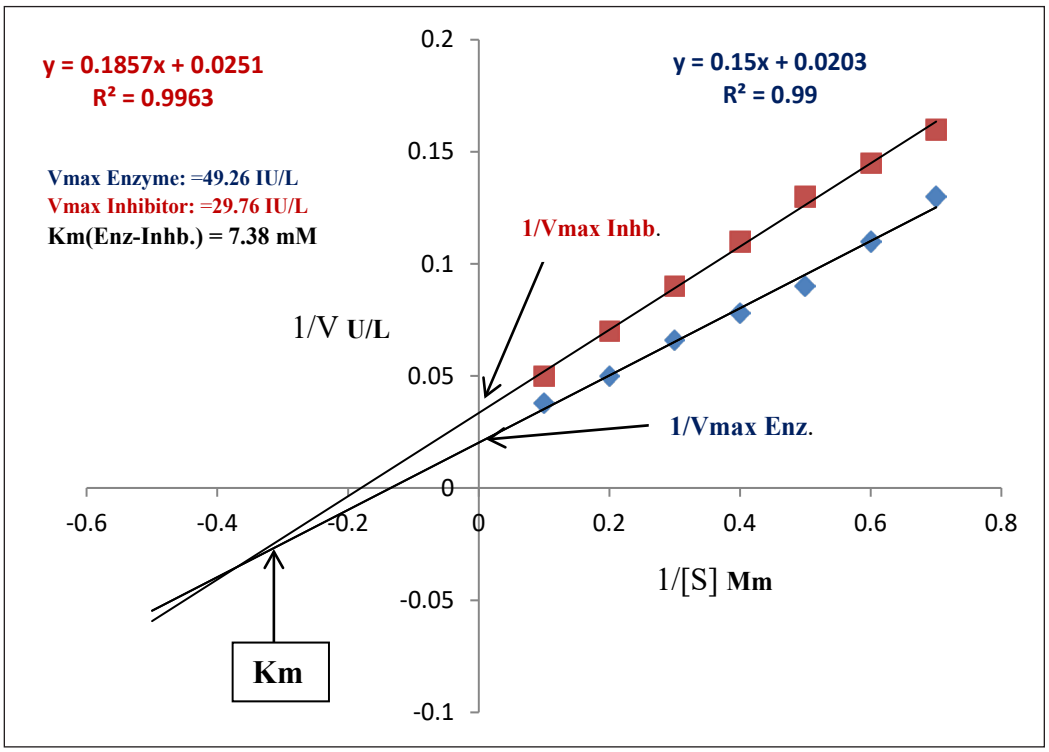

Figure 16. Lineweaver–Burk plot fitting showed that the prepared complex behaves as non-competitive inhibitors. The blue and the red points refer to the inhibitor's absence and presence, respectively

of the enzyme reached the normal value because of the multi dilutions of the concentration of the complex. These results are in agreement with the literature data (Kalita et al., 2018; Oboh et al., 2015). The active site of the amylase enzyme contains amino acids, aspartic acids, glutamic acids, and methionine, which can bind the platinum found in the structure of the complex (inhibitor), thus impeding the ground of the active site with the foundation and leading to inhibition of the amylase activity (Yang et al., 2012). The type of inhibition was shown as non-competitive (*Km* value was fixed:7.38 mM, and the *Vmax* was decreased (Vmax without inhibitor 49.26 IU/L) (*Vmax* with inhibitor 29.76 IU/L) as in Figure 16.

CONCLUSION

We have successfully purified amylase from the serum of patients with T2DM. Several spectroscopic methods prepared and diagnosed inorganic complex derived from vitamin C. Also, a comparison between the experimental and theoretical data was performed. The DFT study of the prepared complex gave a useful explanation of the complex and its stability. Furthermore, the Pt(II) complex showed an inhibitory effect on the amylase activity, which needs further investigation in vivo as a medical drug.

ACKNOWLEDGMENT

Our deep grateful thanks to Department of Chemistry, College of Science. Anbar University for cooperating with us to complete the experimental and to Department of Applied Chemistry, College of Applied Sciences. University of Fallujah for cooperating with us to complete the calculated part.

REFERENCES

Adnan, F. (2010). Kinetics and thermodynamic studies of alpha amylase from *Bacillus licheniformis* mutant. *Pakistan Journal of Botany*, *42*(5), 3507-3516.

Albuquerque, T. L. D., Peirce, S., Rueda, N., Marzocchella, A., Gonçalves, L. R. B., Rocha, M. V. P., & Fernandez-Lafuente, R. (2016). Ion exchange of β-galactosidase: the effect of the immobilization pH on enzyme stability. *Process Biochemistry*, *51*(7), 875–880. https://doi.org/10.1016/j.procbio.2016.03.014

Al-Qodah, Z. (2007). Determination of kinetic parameters of α-amylase producing thermophile *Bacillus sphaericus*. *African Journal of Biotechnology*, *6*(6), 699-706.

Ali, R., Bulat, K. H. K., Azmi, A. A., & Anuar, S. T. (2019). Theoretical approach of dft b3LYP/6-31G (d, p) on evaluating the performance of tert-butylhydroquinone and free fatty acids in inhibiting the oxidation of palm olein. *Journal of Oil Palm Research*, *31*(1), 122-129. https://doi.org/10.21894/JOPR.2019.0005

Ard, D., Tettey, N. S., & Feresu, S. (2020). The influence of family history of type 2 diabetes mellitus on positive health behavior changes among African Americans. *International Journal of Chronic Diseases, 2022*, Article 8016542. https://doi.org/10.1155/2020/8016542

Association, A. D. (2014). Diagnosis and classification of diabetes mellitus. *Diabetes Care*, *37*(Supplement 1), S81-S90. https://doi.org/10.2337/dc14-S081

Bakalova, A., Varbanov, H., Stanchev, S., Ivanov, D., & Jensen, F. (2009). DFT study of the structure and spectral behavior of new pt (II) complexes with 5-methyl-5 (4-pyridyl) hydantoin. *International Journal of Quantum Chemistry*, *109*(4), 826-836. https://doi.org/10.1002/qua.21890

Bergamini, P., Marchesi, E., Bertolasi, V., Fogagnolo, M., Scarpantonio, L., Manfredini, S., Vertuani, S., & Canella, A. (2008). New coordination modes of L-ascorbic acid and dehydro-L-ascorbic acid as dianionic chelating ligand for platinum. *European Journal of Inorganic Chemistry, 2008*(4)*,* 529-537. https://doi.org/10.1002/ejic.200700808

Bradshaw, M. P., Barril, C., Clark, A. C., Prenzler, P. D., & Scollary, G. R. (2011). Ascorbic acid: A review of its chemistry and reactivity in relation to a wine environment. *Critical Reviews in Food Science and Nutrition*, *51*(6), 479-498. https://doi.org/10.1080/10408391003690559

Burhan, A., Nisa, U., Gökhan, C., Ömer, C., Ashabil, A., & Osman, G. (2003). Enzymatic properties of a novel thermostable, thermophilic, alkaline and chelator resistant amylase from an alkaliphilic *Bacillus* sp. isolate ANT-6. *Process Biochemistry*, *38*(10), 1397-1403. https://doi.org/10.1016/S0032-9592(03)00037-2

Caruso, F., Rossi, M., Benson, A., Opazo, C., Freedman, D., Monti, E., Gariboldi, M. B., Shaulky, J., Marchetti, F., & Pettinari, R. (2012). Ruthenium-arene complexes of curcumin: X-ray and density functional theory structure, synthesis, and spectroscopic characterization, in vitro antitumor activity, and DNA docking studies of (p-cymene) Ru (curcuminato) chloro. *Journal of Medicinal Chemistry*, *55*(3), 1072-1081. https://doi.org/ 10.1021/jm200912j

Chattaraj, P. K., & Poddar, A. (1999). Molecular reactivity in the ground and excited electronic states through density-dependent local and global reactivity parameters. *The Journal of Physical Chemistry A*, *103*(43), 8691-8699. https://doi.org/10.1021/JP991214+

Chen, L., Strohmeier, V., He, Z., Deshpande, M., Catalan-Dibene, J., Durum, S. K., Moran, T. M., Kraus, T., Xiong, H., & Faith, J. J. (2019). Interleukin 22 disrupts pancreatic function in newborn mice expressing IL-23. *Nature Communications*, *10*, Article 4517. https://doi.org/10.1038/s41467-019-12540-8

Czarnomysy, R., Surażyński, A., Muszynska, A., Gornowicz, A., Bielawska, A., & Bielawski, K. (2018). A novel series of pyrazole-platinum (II) complexes as potential anti-cancer agents that induce cell cycle arrest and apoptosis in breast cancer cells. *Journal of Enzyme Inhibition and Medicinal Chemistry*, *33*(1), 1006-1023. https://doi.org/10.1080/14756366.2018.1471687

Dhote, Y. S., Moharil, M. P., & Jadhav, P. V. (2014). Isolation and characterization of amylase inhibitor from alkalophilic bacteria isolated from lonar crater and its insecticidal protein producing ability. *Biosciences, Biotechnology Research Asia*, *11*(1), 329-333.

Duong-Ly, K. C., & Gabelli, S. B. (2014). Salting out of proteins using ammonium sulfate precipitation. *Methods in Enzymology*, *541*, 85-94. https://doi.org/10.1016/B978-0-12-420119-4.00007-0

Egan, A. M., & Dinneen, S. F. (2019). What is diabetes? *Medicine*, *47*(1), 1-4. https://doi.org/10.1016/J.MPMED.2018.10.002

Elghalban, M. G., El Defarwy, A. M., Shah, R. K., & Morsi, M. A. (2014). α-Furil dioxime: DFT exploration and its experimental application to the determination of palladium by square wave voltammetry. *International Journal of Electrochemical Science, 9*, 2379-2396.

Halim, M., & Halim, A. (2019). The effects of inflammation, aging and oxidative stress on the pathogenesis of diabetes mellitus (type 2 diabetes). *Diabetes & Metabolic Syndrome: Clinical Research & Reviews*, *13*(2), 1165-1172. https://doi.org/10.1016/j.dsx.2019.01.040

Hames, B. D. (1998). *Gel electrophoresis of proteins: A practical approach* (3rd Ed.). OUP Oxford.

Hollis, L. S., Stern, E. W., Amundsen, A. R., Miller, A. V, & Doran, S. L. (1987). Platinum complexes of vitamin C. NMR studies on the solution chemistry of cis-platinum (diamine)(ascorbate) complexes. *Journal of the American Chemical Society*, *109*(12), 3596-3602. https://doi.org/10.1021/ja00246a016

Hong, H. R., Oh, Y. I., Kim, Y. J., & Seo, K. W. (2019). Salivary alpha-amylase as a stress biomarker in diseased dogs. *Journal of Veterinary Science*, *20*(5), Article e46. https://doi.org/10.4142/jvs.2019.20.e46

Kalita, D., Holm, D. G., LaBarbera, D. V, Petrash, J. M., & Jayanty, S. S. (2018). Inhibition of α-glucosidase, α-amylase, and aldose reductase by potato polyphenolic compounds. *PLoS One*, *13*(1), Article e0191025. https://doi.org/10.1371/journal.pone.0191025

Kumar, S., & Chakravarty, S. (2018). Amylases. In *Enzymes in Human and Animal Nutrition* (pp. 163-180). Elsevier.

López, J. L., Alvarez, F., Príncipe, A., Salas, M. E., Lozano, M. J., Draghi, W. O., Jofré, E., & Lagares, A. (2018). Isolation, taxonomic analysis, and phenotypic characterization of bacterial endophytes present in alfalfa (*Medicago sativa*) seeds. *Journal of Biotechnology*, *267*, 55-62. https://doi.org/10.1016/j.jbiotec.2017.12.020

Maher, F. T., Mukhlis, A. J., Abuod, A. I., & Naji, N. A. (2017). *In vivo* study of compounds 3-(acetyl Salicyloyl)-5, 6–Oisopropylidene-L-ascorbic acid, 2, 3-(acetyl Salicyloyl)-5, 6–O-isopropylidene-L-ascorbic acid and 2, 3, 5, 6Tetra (acetyl Salicyloyl)-L-ascorbic acid. *Ibn Al-Haitham Journal for Pure and Applied Science*, *22*(2), 1-7.

Mahmood, N. (2016). A review of α-amylase inhibitors on weight loss and glycemic control in pathological state such as obesity and diabetes. *Comparative Clinical Pathology*, *25*, 1253-1264. https://doi.org/10.1007/s00580-014-1967-x

Mansour, A. M. (2013). Coordination behavior of sulfamethazine drug towards Ru (III) and Pt (II) ions: Synthesis, spectral, DFT, magnetic, electrochemical and biological activity studies. *Inorganica Chimica Acta*, *394*, 436-445. https://doi.org/10.1016/j.ica.2012.08.025

McGuire, J. P., Friedman, M. E., & McAuliffe, C. A. (1984). Studies of enzyme inhibition. The interaction of some platinum (II) complexes with fumarase and malate dehydrogenase. *Inorganica Chimica Acta*, *91*(3), 161-165. https://doi.org/10.1016/S0020-1693(00)81806-X

Mistry, B. D. (2009). *A handbook of spectroscopic data: Chemistry*. Oxford.

Mohhmod, R. J. (2010). Kinetics of α-amylase enzyme inhuman serum. *Journal of Kerbala University*, *8*(3), 237-244.

Oboh, G., Agunloye, O. M., Adefegha, S. A., Akinyemi, A. J., & Ademiluyi, A. O. (2015). Caffeic and chlorogenic acids inhibit key enzymes linked to type 2 diabetes (in vitro): A comparative study. *Journal of Basic and Clinical Physiology and Pharmacology*, *26*(2), 165-170. https://doi.org/10.1515/jbcpp-2013-0141

Oboh, G., Isaac, A. T., Akinyemi, A. J., & Ajani, R. A. (2014). Inhibition of key enzymes linked to type 2 diabetes and sodium nitroprusside induced lipid peroxidation in rats' pancreas by phenolic extracts of avocado pear leaves and fruit. *International Journal of Biomedical Science*, *10*(3), 208-216.

Romero-Canelon, I., & Sadler, P. J. (2013). Next-generation metal anticancer complexes: multitargeting via redox modulation. *Inorganic Chemistry*, *52*(21), 12276-12291. https://doi.org/10.1021/ic400835n

Sabounchei, S. J., Shahriary, P., Salehzadeh, S., Gholiee, Y., Nematollahi, D., Chehregani, A., Amani, A., & Afsartala, Z. (2015). Pd (II) and Pd (IV) complexes with 5-methyl-5-(4-pyridyl) hydantoin: Synthesis, physicochemical, theoretical, and pharmacological investigation. *Spectrochimica Acta Part A: Molecular and Biomolecular Spectroscopy*, *135*, 1019-1031. https://doi.org/10.1016/j.saa.2014.08.002

Salomon, L. L. (1963). Preparation of 5, 6-O-isopropylidene-L-ascorbic acid. *Experientia*, *19*(12), 619-620. https://doi.org/10.1007/BF02151276

Silano, V., Barat Baviera, J. M., Bolognesi, C., Cocconcelli, P. S., Crebelli, R., Gott, D. M., Grob, K., Lambré, C., & Lampi, E. (2020). Safety evaluation of the food enzyme α-amylase from the genetically modified *Bacillus licheniformis* strain DP-Dzb45. *EFSA Journal*, *17*(6), Article e06311. https://doi.org/10.2903/j.efsa.2019.5738

Silverstein, R. M., Webster, F. X., & Kiemle, D. J. (2005). *Spectrometric Identification of Organic Compounds, 7th Edition.* John Wiley & Sons. Inc.

Soliman, A. A., Alajrawy, O. I., Attaby, F. A., & Linert, W. (2016). New binary and ternary platinum (II) formamidine complexes: Synthesis, characterization, structural studies and in-vitro antitumor activity. *Journal of Molecular Structure*, *1115*, 17-32. https://doi.org/10.1016/J.MOLSTRUC.2016.02.073

Tilley, L. P., & Smith Jr, F. W. K. (2015). *Blackwell's five-minute veterinary consult: Canine and feline*. John Wiley & Sons.

Varley, H., Gowenlock, A. H., McMurray, J. R., & McLauchlan, D. M. (1988). *Varley's practical clinical biochemistry*. Heinemann Medical Books.

Whitcomb, D. C., & Lowe, M. E. (2007). Human pancreatic digestive enzymes. *Digestive Diseases and Sciences*, *52*(1), 1-17. https://doi.org/10.1007/s10620-006-9589-z.

Yαlçın, G. (1995). Studies on cis-DDP,[Pt (Dach)(MePhSO) Cl]+ and [Pt (NH3) 2 (N-Py) Cl]+ binding to fumarase. *Drug Metabolism and Drug Interactions*, *12*(2), 105-116. https://doi.org/10.1515/DMDI.1995.12.2.105.

Yang, H., Liu, L., Wang, M., Li, J., Wang, N. S., Du, G., & Chen, J. (2012). Structure-based engineering of methionine residues in the catalytic cores of alkaline amylase from *Alkalimonas amylolytica* for improved oxidative stability. *Applied and Environmental Microbiology*, *78*(21), 7519-7526. https://doi.org/10.1128/AEM.01307-12

Yu, H. (2019). *Kiwifruit effects on starch digestion by salivary amylase under simulated gastric conditions* (Master dissertation). University of Otago, New Zealand. http://hdl.handle.net/10523/9448

Zhao, Y., Ouyang, X., Chen, J., Zhao, L., & Qiu, X. (2018). Separation of aromatic monomers from oxidatively depolymerized products of lignin by combining Sephadex and silica gel column chromatography. *Separation and Purification Technology*, *191*, 250-256. https://doi.org/10.1016/j.seppur.2017.09.039

Zümreoglu-Karan, B. (2006). The coordination chemistry of vitamin C: An overview. *Coordination Chemistry Reviews*, *250*(17-18), 2295-2307. https://doi.org/10.1016/j.ccr.2006.03.002